Arab J Sci Eng
DOI 10.1007/s13369-013-0815-7

RESEARCH ARTICLE - CIVIL ENGINEERING

Seismic Evaluation of the ACI Code Provisions for Lap Splicing of Longitudinal Bars in R/C Rectangular Bridge Columns

Mohammad S. Al Haddad · Hussein M. Elsanadedy · Rizwan A. Iqbal

Received: 24 March 2012 / Accepted: 24 July 2013

Abstract In this study, the adequacy of the ACI code provisions for detailing of lap-spliced reinforcement in R/C rectangular bridge columns was numerically investigated. Pushover analysis was conducted on a total of 324 R/C rectangular bridge columns with lap-spliced reinforcement, using a modified version of previously developed computer program. The computer modeling is based on moment–curvature analysis of the column section with the inclusion of a bond/slip mechanism and concrete confinement model. In this study, the program was revised to integrate the effectiveness of lateral hoop reinforcement on both concrete confinement and lap-splice clamping. Constant axial load was applied in the analysis. The parameters involved in the study were lap-splice length, volumetric ratio of column hoops, and axial load ratio. The results indicate that the top lateral load–displacement characteristics of the column are enhanced when the lap-splice length at the column base increased. To ensure a minimum displacement ductility of 4.0 for the column, lap splices as short as $30\phi_b$ (ϕ_b = longitudinal bar-diameter) should be avoided at expected plastic hinge locations. The best performance for a wide range of axial load ratios was exhibited by columns having the ACI's classes A and B tension splices and laterally reinforced with hoops required by the ACI code for seismic design.

Keywords R/C bridge columns · Lap-splice reinforcement · Pushover analysis

الخلاصة

تـم فـى هـذا البحـث تقيـيم مـدى كفايـة إشـتراطات الكـود الأمريكـى (ACI code) الخاصة بتفاصيل وصلات التراكب فى حديد التسليح الطولى لأعمدة الجسور الخرسانية المسلحة مستطيلة المقطع. حيث تم إجراء تعديل لبرنامج كومبيوتر قائم لإستخدامه فى عمل تحليل الدفع الجانبى لعدد 324 عمود جسر خرساني مستطيل المقطع وذو وصلات تراكب عند إلتقائه بالقاعدة. ويعتمد النموذج الرياضي على عمل تحليل العزوم والدوران لمقطع العمود حيث تم تعديل البرنامج ليأخذ فى الإعتبار تأثير كانات العمود الأفقية على كل من وصلات التراكب فى الشد وسلوك الخرسانة فى منطقة الضغط. وقد تم تثبيت قوة الضغط المحورية على مقطع العمود أثناء التحليل الرياضي. لقد شملت نقاط الدراسة فى هذا البحث على كل من: طول وصلات التراكب ونسبة حجم الكانات بالإضافة إلى نسبة القوى المحورية. وقد أظهرت النتائج أن زيادة طول وصلات التراكب قد حسّن من خصائص منحنى الحمل والإزاحة الأفقية وللحصول على ممطولية أكبر من أو تساوى 4 يجب تجنب إستخدام وصلات تراكب بطول أقل من أو يساوى 30 مرة قطر السيخ. إن أحسن أداء لمدى واسع من نسبة التحميل المحورى كان لأعمدة لها وصلات تراكب من الفئة (A) والفئة (B) فى الشد (حسب مواصفات الكود الأمريكى للخرسانة) والتى تم تسليحها بكانات أفقية تقاوم أحمال الزلازل طبقاً للكود الأمريكى للخرسانة ACI318.

1 Introduction

Lap splices in R/C elements, if not carefully detailed, may be locations of potential damage especially when exposed to fully reversed cyclic loadings of short-duration excitations such as seismic loads and blast. It can be said that in most high bridges all over the world the longitudinal reinforcement of the columns is spliced with starter bars extending from the column footing. In addition, in the old bridges built in the 1960's and in the early 1970's, lap splices at the column base are of the compression type with lengths as short as 20 times the bar-diameter (see Fig. 1). Apart from this, in some cases, transverse column reinforcement with substandard hoops of insufficient volumetric ratio for even gravity-loaded columns was engaged [1].

M. S. Al Haddad · H. M. Elsanadedy (✉) · R. A. Iqbal
Department of Civil Engineering, King Saud University, Riyadh, Saudi Arabia
e-mail: elsanadedy@yahoo.com

Published online: 07 September 2013

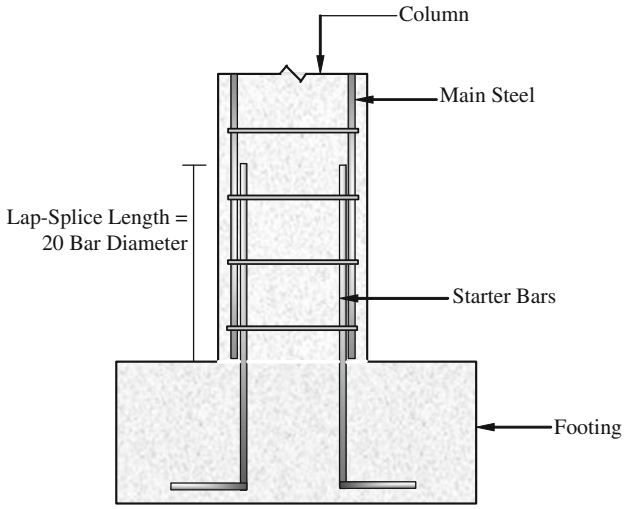

Fig. 1 Lap-splice details in older bridge columns

Lap splices in tall bridge columns and at the base of multistory buildings located in the potential plastic hinge zones, if poorly detailed, will experience severe damage under seismic actions. Furthermore, under reversed cyclic loading, the transverse reinforcement may not provide adequate confinement for the core concrete under compression and sufficient clamping action to the lap splice to prevent de-bonding. The concrete cover may therefore start to spall prematurely and anchorage of the lapped bars may degrade rapidly due to the splitting action under fully reversed cyclic loads. Consequently, the ductility capacity of the reinforced concrete columns is greatly reduced, which may cause brittle failure. Lessons learned from past major earthquakes indicate that this kind of brittle failure in the lap-splice zone caused a total or partial collapse of columns. Cases depicted by pictures of such failures in both building and bridge piers are shown in Fig. 2.

Fig. 2 Lap-splice failure at base of building and bridge columns

(a) Turkey Earthquake, 1999

(b) Kobe Earthquake, 1995

(c) Kobe Earthquake, 1995

In this study, a FORTRAN-based computer program was modified to include the effect of lateral hoop reinforcement on both concrete confinement and lap-splice clamping. The unique aspect of this program was the integration of bond–slip mechanism and the concrete confinement model for the moment–curvature analysis of column sections. The ACI code seismic provisions which are mainly developed for building columns have also been evaluated in this study for adequacy in providing details of lap-spliced reinforcement in R/C rectangular bridge columns.

1.1 ACI Code Provisions

As per the ACI 318-11 code [1], there are two classes of tension lap splices—Class A and Class B. The length of the tension lap is a function of the tension development length, l_d, as follows:

- Class A splice: 1.0 l_d
- Class B splice: 1.3 l_d

The ACI code states that lap splices of deformed bars in tension shall be Class B splices except that Class A splices are allowed when (a) the area of reinforcement provided is at least twice that required by analysis over the entire length of the splice, and (b) one-half or less of the total reinforcement is spliced within the required lap length. If the column is expected to experience lateral loading (such as earthquakes or blast attacks), the lap splice should be designed as a Class B tension splice since all column bars are usually spliced at the same location.

For the volumetric ratios of hoop reinforcement, the seismic codes such as Caltrans design guidelines [2] and the ACI 318-11 [1] provide the following provisions for R/C rectangular columns:

- The total area of rectangular hoops shall not be less than that required by Eqs. (1) and (2).

$$A_{sh} = 0.3 s h_c \frac{f'_c}{f_{yh}} \left[\frac{A_g}{A_{ch}} - 1 \right] \tag{1}$$

$$A_{sh} = 0.09 s h_c \frac{f'_c}{f_{yh}} \tag{2}$$

where A_{sh} = total cross-sectional area of transverse reinforcement (including crossties) within spacing s and perpendicular to dimension h_c, mm^2; s = spacing of transverse reinforcement measured along the longitudinal axis of the column, mm; h_c = cross-sectional dimension of column core measured center-to-center of confining reinforcement, mm; f'_c = specified cylinder compressive strength of concrete, MPa; f_{yh} = specified yield strength of transverse reinforcement, MPa; A_g = gross area of column section, mm^2; and A_{ch} = area of column core measured out-to-out of transverse reinforcement, mm^2.

- Transverse reinforcement shall be spaced at a distance not exceeding (a) one-quarter of the minimum member dimension, (b) six times the diameter of the longitudinal reinforcement, and (c) s_x as defined by Eq. (3).

$$s_x = 100 + \left(\frac{350 - h_x}{3} \right) \tag{3}$$

where h_x = maximum horizontal spacing of hoop or crosstie legs on all faces of the column, mm. The value of s_x shall not exceed 150 mm and does not need to be less than 100 mm.

- Crossties or legs of overlapping hoops shall not be spaced more than 350 mm on center in the direction perpendicular to the longitudinal axis of the column.

1.2 Background Literature Review

Experimental investigations [3–14] were carried out by some researchers to study the seismic performance of tall bridge columns with lap-spliced reinforcement. Sun et al. [3] tested two large-scale rectangular bridge columns with poor lap-splice details. Both columns were exposed to constant axial load ratio (ratio between applied axial load and axial capacity of the column) of 0.15 and lateral cyclic loading about their strong and weak axes, respectively. The two columns failed prematurely due to slippage at the lap-splice zone.

Chung et al. [4] carried out a study to evaluate the seismic performance of circular bridge piers with spliced longitudinal steel in the plastic hinge region, to develop the enhancement scheme for their seismic capacity by retrofitting with glass fiber sheet and also the appropriate limited ductility design concept in low and moderate seismicity regions. Quasi-static tests were conducted on nine test specimens in a displacement-controlled way under three different axial load levels. Results of this study indicated that non-seismically designed columns with lap splices in the potential plastic hinge regions appeared to fail at low ductility levels. This was attributed to the de-bonding of lap splices which resulted from insufficient development length of the longitudinal bars. Test columns externally wrapped with glass fiber sheets showed significant improvement in the displacement ductility.

In a study, Kim et al. [5] assessed the seismic performance of R/C bridge piers with lap splices in longitudinal reinforcing bars in order to provide data for developing improved seismic design criteria. A method for analyzing the nonlinear hysteretic behavior and ductility capacity of R/C bridge piers with lap splices under earthquakes was proposed. A computer program, Reinforced Concrete Analysis in Higher

Evaluation System Technology (RCAHEST), was used to analyze R/C structures. A lap-spliced bar element was newly developed to predict the inelastic behaviors of lap splices. The proposed numerical method was then verified by comparing it with test data developed by the authors. The authors finally concluded that the proposed model described the inelastic behavior of the bridge pier with reasonable accuracy. It is not desirable to permit the lap splice of longitudinal bars in the potential plastic hinge zone without increasing the transverse confinement, in a moderate seismic region.

Experimental tests were carried out by Chung et al. [6] to evaluate the seismic ductility of previously damaged R/C columns. The test parameters included confinement ratio, lap splice of longitudinal steel, and retrofitting fiber-reinforced polymer (FRP) materials. The research objective was to subject R/C bridge piers to artificial earthquake using a pseudo-dynamic test (PDT), and then to examine their seismic performance in a quasi-static test (QST). Test results depicted that except for the ordinary specimens with lap-spliced longitudinal bars, most specimens pre-damaged during the PDT generally demonstrated good residual seismic performance. Test results also indicated that R/C piers retrofitted with fiber composite wraps in the potential plastic hinge region exhibited enhanced flexural ductility. It was concluded that lap-spliced R/C piers are especially vulnerable and need to be retrofitted to secure good seismic performance in subsequent earthquakes.

Haroun [7] and Elsanadedy [8] conducted a testing program on scaled models of R/C bridge columns with insufficient lap-splice length. Three columns were tested in the as-built configuration whereas ten specimens were tested after being retrofitted with different FRP jacket systems. A brittle failure was observed in the as-built columns due to bond deterioration of the lap-spliced longitudinal reinforcement. The FRP-jacketed circular columns demonstrated a significant improvement in their cyclic performance. Yet, tests conducted on square-jacketed columns showed a limited improvement in clamping on the lap-splice region and for enhancing the ductility of the column.

Bousias et al. [9,10] tested 45 rectangular columns, with plain and deformed vertical bars subjected to cyclic flexure with constant axial load. Test parameters included the presence and length of lap splices and the type of retrofitting: concrete jackets over the whole column, or CFRP wrapping of the plastic hinge region at varying number of layers and height of application from the base. The test results of the un-retrofitted ribbed-type columns showed that old-type columns with ribbed bars lap-spliced at the base have reduced cyclic deformation capacity and energy dissipation. Lapping of straight ends of ribbed bars by as little as 15 bar-diameters reduces appreciably flexural resistance and gives rapid post-peak strength and stiffness degradation and low energy dissipation capacity. It was concluded that in columns with ribbed bars, FRP wrapping cannot fully remove the adverse effects on force capacity and energy dissipation of a very short lapping of straight bar ends (e.g. in the order of 15 bar-diameters) near the base. Also, in columns with straight ribbed bars even R/C jacketing cannot fully re-instate the cyclic deformation capacity and energy dissipation to that of a monolithic column, if the original column has very short lapping, e.g. $15\phi_b$.

In two other studies by Chang et al. [11,12] more than 60 large-scale circular and rectangular columns were tested, including specimens which were designed to represent columns constructed in Taiwan before and after 1987. Worst details for lap splice at plastic hinge locations expected in bridge columns were assumed in these test specimens. The results of testing un-retrofitted columns were compared with columns retrofitted with CFRP jackets, steel jackets, and R/C jackets. Tests indicated that due to the poor compressive strength of concrete and the lap splicing at plastic hinge zone, the retrofit measures developed for better ductility and shear strength are not always effective. It was concluded that applying CFRP directly cannot provide enough confinement stress to increase frictional force between the lap-spliced longitudinal reinforcements.

Testing of rectangular columns with a lap-splice length of $40\phi_b$ in the plastic hinge zone was carried out [11]. The failure of lap-spliced columns at low ductility of 1.5 and 2.0 was caused by the bond failure at the splices of longitudinal bars.

ElGawady et al. [13] investigated the cyclic behavior of eight 0.4-scale R/C columns. The columns incorporated deficient design details to simulate bridge columns built in Washington prior to 1971. CFRP as well as steel jacketing were incorporated as retrofitting of the columns along with un-retrofitted columns used as reference specimens. The columns were tested under constant gravity loads and incremental increase in lateral load cycles. It was noticed that the as-built specimens had two modes of failures, namely low cyclic fatigue of longitudinal reinforcement and lap-splice failure. For the retrofitted specimens, no lap-splice failure was observed. All the retrofitted specimens failed due to low cyclic fatigue failure of the longitudinal bars which is caused as a result of large tension and compression strain reversals of typically 1–5 reversed equi-amplitudes in the rebars. The retrofitting measures improved the displacement ductility, energy dissipation, and equivalent viscous damping.

Another study by Ghosh and Sheikh [14] focused on the seismic upgrade of existing R/C columns detailed with poor lap splices and inadequate transverse confinement reinforcement in the potential plastic hinge regions. A total of 12 columns were subjected to simulated earthquake loading. The variables studied in the program included the effect of the presence of lap splices, the effectiveness of CFRP in pre-earthquake strengthening and post-earthquake retrofitting of deficient columns, as well as the effects of level of axial load,

shape of column cross section, and transverse steel details. This study concluded that poorly detailed lap splices in the plastic hinge region resulted in significant reduction in ductility and unstable hysteretic behavior along with rapid degradation in strength due to premature splice failure. Retrofitting of columns with CFRP resulted in improved ductility and strength behavior and the level of improvement, however, would be dependent on the damage experienced by the column prior to retrofitting.

In the current study, pushover analysis was carried out on full-scale rectangular tall bridge columns with lap splices at their base. Constant axial loads were applied in the analysis. The parametric study variables included lap-splice length, volumetric ratio of column hoops, and axial load ratio. The studied response parameters included load–displacement characteristics, column displacement ductility, and ultimate slip and elongation strains for extreme tension bars.

2 Pushover Analysis

Pushover analysis of R/C rectangular columns with lap-spliced reinforcement was conducted in this study using an object-oriented computer program which was previously developed by one of the authors in an earlier study [7]. The computer program which is written in the FORTRAN 90 language was modified to be used in this research. The program is based on moment–curvature analysis of the column section with the inclusion of a bond/slip mechanism and concrete confinement model. Since the program was originally developed for columns confined with FRP jackets, it had to be revised to include the effectiveness of the lateral hoop reinforcement on both concrete confinement and lap-splice clamping. This simple tool would then be able to help structural engineers conduct pushover analysis on R/C rectangular bridge columns with lap-spliced reinforcement and having different volumetric ratios of lateral hoops. The column input data such as column dimensions, reinforcement details, lap-splice length, concrete compressive strength, yield strength of reinforcing steel, and axial load are read into the program via an input text file. The output text file is created upon running the program and it includes analysis results for moment–curvature calculations, history of bar slip strain, and load–displacement curve.

2.1 Approach and Assumptions

In defining the constitutive properties of the materials, concrete is of important concern. In this case concrete was ignored in tension after cracking. However, for concrete in compression, it was considered laterally confined by hoop reinforcement. A laminar approach was used to analyze the column. The moment–curvature relationship was determined by increasing the strain in the extreme compression fiber of the column section in increments up to the ultimate concrete compressive strain. For each increment, the strain at the extreme tensile steel bar was assumed. The assumption of plane section remains plane was made so that a linear strain distribution across the column section was assumed. The stresses in each concrete layer were calculated using the stress–strain relationship of concrete, once the strains in concrete were obtained from the program. The force resultant in each concrete layer was then determined. It was further assumed that bond stress is uniformly distributed along the length of bond links and the nonlinear effects could be ignored. The total geometric strain for each bar in tension consisted of two components: slippage and elongation. By using bond–slip relationship and the stress–strain model for the steel, an iterative procedure was performed for each bar to satisfy the equilibrium condition. After that, slippage of each bar in tension was determined and the stresses were computed. Thereby, the tensile forces for all bars were estimated. The use of convergence criteria assured the equilibrium of internal forces for the entire section. Axial force convergence allowed both the moment resultants on the column and the section curvature to be determined.

The moment–curvature curve of the column section was transformed into load–displacement history from zero up to failure by conducting the pushover analysis of the bridge column. In estimating the lateral displacement of the column, the flexural deformation was computed by integrating the curvature distribution along the column length. For ease, two elastic segments represented curvature distribution up to the first yield of the longitudinal steel: one corresponded to the uncracked concrete section and the other to the cracked section. Curvature was assumed constant along the plastic hinge length after yielding.

Ductility in a structure is defined as the ability to deform in the plastic region at previously designated hinge locations without significant strength degradation. The column displacement ductility factor was calculated from the following equation.

$$\text{Ductility factor} = \frac{\Delta_u}{\Delta_y} \tag{4}$$

where Δ_u = ultimate displacement calculated at ultimate limit state and Δ_y = idealized yield displacement. In the analysis of lap-splice columns, the ultimate limit state was defined as that corresponding to whichever of the following occurs first:

- Ultimate concrete compression strain ε_{cu} (depends on parameters in Eq. (8)).
- Maximum longitudinal reinforcement tensile strain, taken as $0.7\varepsilon_{su}$, where ε_{su} is the ultimate strain of reinforcing steel taken as 0.12.

- Maximum slip strain of 0.10 in the extreme longitudinal tension bar.
- Post-peak load of 80 % of the maximum lateral load.

The idealized yield displacement was calculated from the following equation

$$\Delta_y = \frac{F_i}{F_y}\Delta_1 \tag{5}$$

where Δ_1 is the displacement corresponding to the first-yield lateral load, F_y. The ideal flexural lateral load capacity, F_i, was computed based on the extreme concrete compressive strain of 0.005 [15].

2.2 Stress–Strain/Strength Models

Mander's model for steel-confined concrete [16] was employed in the program. According to Mander's model, the confined concrete compressive strength is given by

$$f'_{cc} = f'_c\left[2.254\sqrt{1+\frac{7.94f_l}{f'_c}} - \frac{2f_l}{f'_c} - 1.254\right] \tag{6}$$

and the strain at maximum concrete stress is estimated from

$$\varepsilon_{cc} = 0.002\left[1+5\left(\frac{f'_{cc}}{f'_c}-1\right)\right] \tag{7}$$

whereas, the ultimate concrete compressive strain, defined as strain at first hoop fracture, is given by the following formula, proposed by Priestley et al. [17]:

$$\varepsilon_{cu} = 0.004 + \frac{1.25\rho_v f_{yh}\varepsilon_{su}}{f'_{cc}} \tag{8}$$

where ρ_v = volumetric ratio of lateral hoops, f_{yh} = yield strength of lateral hoops, and ε_{su} = ultimate strain of lateral hoops. The lateral confining stress on the concrete (total transverse bar force divided by vertical area of confined concrete) is calculated from

$$f_l = \frac{1}{2}k_e f_{yh}\left(\frac{A_{sx}}{sh_c} + \frac{A_{sy}}{sb_c}\right) \tag{9}$$

where, A_{sx} and A_{sy} = the total area of transverse bars running in the 'x' and 'y' directions, respectively; s = center-to-center spacing of lateral hoops; and k_e is the confinement effective coefficient as given in Mander's model [16].

In addition to defining the stress–strain characteristics of concrete, a model of the stress–strain properties of steel reinforcement [7] was also employed in the program. This model was divided into three major zones: a linear portion up to the yield point, a yield plateau region, and a parabolic strain-hardening curve. The yield strain (ε_y) is considered as the strain corresponding to the yield strength depending on the grade of rebar used; the strain hardening was considered to start at $\varepsilon_{sh} = 5\varepsilon_y$ and the ultimate strain (ε_{su}) was taken as 0.12. In the analytical model, bond/slip of the lap-spliced longitudinal bars was also taken into consideration. Three different bond/slip models are available in the program of which the model developed by Xiao et al. [15] (see Fig. 3) was utilized in this study, since it was found to give good correlation with numerous experimental data [7].

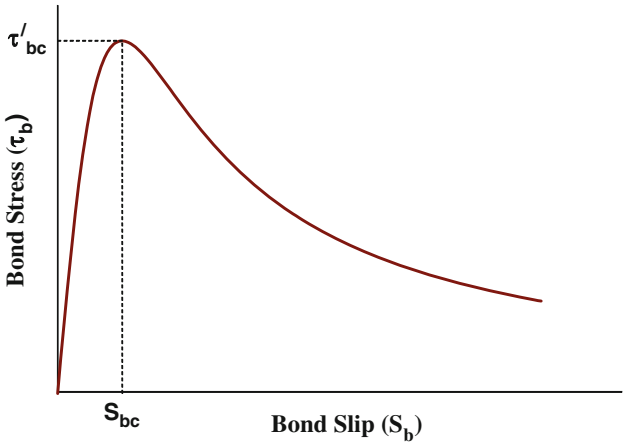

Fig. 3 Xiao's bond–slip model [15]

In the Xiao's model, the bond–slip relationship is given by the following empirical equation:

$$\tau_b = \frac{\tau'_{bc} r(S_b/S_{bc})}{r-1+(S_b/S_{bc})^r} \tag{10}$$

where τ'_{bo} = peak bond stress between the steel bar and confined concrete, and is given by

$$\tau'_{bc} = \tau'_{bo} + 1.4f_l \tag{11}$$

where τ'_{bo} = bond strength for steel bars in plain unconfined concrete, and is calculated based on the bond strength given by the equation in ACI 408R-03 Committee report [18]:

$$\tau'_{bo} = 20\sqrt{f'_c}/d_{bl} \le 5.52\,\text{MPa} \tag{12}$$

The parameter S_{bc} is the bond/slip corresponding to τ'_{bo}; and is calculated from

$$S_{bc} = S_{bo}\left(1+\alpha\frac{f_l}{f'_c}\right) \tag{13}$$

where S_{bo} =0.254 mm and α = 75.0. The parameter 'r' defines the shape of the curve expressed by Eq. (10), for different transverse confinement and is estimated from

$$r = r_o - k_r\frac{f_l}{f'_c} \tag{14}$$

where r_o = 2.0 and k_r = 13.0. It should be pointed that the value of 'r' calculated using Eq. (14) should be limited to be $r^3 \ge 1.0$.

For the steel bars in compression, the strain at each bar location was computed, and using the stress–strain model for the steel, the stresses were calculated, and hence the force

Table 1 Details of column specimens used for model verification

Col. ID	Column dimensions			Axial load (kN)	$f_c^{'}$ (MPa)	Longitudinal steel			Transverse steel		Source
	Width (mm)	Depth (mm)	Height (mm)			No. and size	f_y (MPa)	Lap length (mm)	size and spacing	f_{yh} (MPa)	
RC(1)	489	730	3,658	1,779	30.5	32 Ø19	315	381	Ø6 @ 127 mm	352	Sun et al. [3]
RC(2)	730	489	3,658	1,779	33.1	32 Ø19	315	381	Ø6 @ 127 mm	352	Sun et al. [3]
RC(3)	610	610	3,658	832	41.4	28 Ø19	444	381	Ø6 @ 127 mm	448	Haroun and Elsanadedy [8]
RC(4)	457	457	1,829	1,601	36.0	8 Ø25	510	508	Ø10 @ 305 mm	481	Melek and Wallace [19]
RC(5)	457	457	1,676	1,068	35.0	8 Ø25	510	508	Ø10 @ 305 mm	481	Melek and Wallace [19]
RC(6)	457	457	1,524	1,601	35.0	8 Ø25	510	508	Ø10 @ 305 mm	481	Melek and Wallace [19]

in each bar was determined. For the steel bars in tension, based on the Xiao et al. [15] model, it was assumed that the stresses in the starter bars are transferred to the longitudinal bars through a series of shear springs.

2.3 Analytical Model Verification

In order to validate the employed numerical models for the prediction of performance of R/C rectangular lap-splice columns, the experimental results of six columns, tested in a single-curvature configuration, have been collected from the literature. The columns were tested by Sun et al. [3], Haroun and Elsanadedy [8], and Melek and Wallace [19]. Details of test columns are illustrated in Table 1. Experimental and numerical results of the six specimens in terms of peak lateral load and lateral drift at peak lateral load are listed in Table 2. Ratios of experimental to predicted values along with their statistical parameters are also shown in Table 2. As demonstrated in the table, the predicted values have good correlation with the experimental results. The full load–displacement envelopes were theoretically predicted and then compared with the experimental curves for columns RC(1)–RC(3), as seen in Fig. 4. Experimental load–displacement envelopes for other columns RC(4)–RC(6) could not be obtained. As identified in Fig. 4, good agreement was achieved between the experimental and predicted curves. This clearly verifies the accuracy of the used numerical models in predicting the behavior of R/C rectangular columns with lap splices at their base.

Table 2 Comparison of experimental and theoretical results for columns used in model verification

Col ID	Peak lateral load (kN)			Drift ratio at peak lateral load (%)		
	EXP	TH	EXP/TH	EXP	TH	EXP/TH
RC(1)	302	307	0.98	0.65	0.69	0.94
RC(2)	265	249	1.06	1.39	1.41	0.98
RC(3)	243	239	1.02	1.02	0.99	1.03
RC(4)	285	281	1.02	1.45	1.39	1.05
RC(5)	270	261	1.03	1.33	1.26	1.06
RC(6)	341	335	1.02	1.50	1.57	0.96
Average			1.02			1.00
Std. Dev.			0.03			0.05
COV			0.02			0.04

3 Selection of Case Studies

A tall rectangular column as part of a single bridge column bent was selected as a case study for pushover analysis in this paper. Figure 5 shows the dimensions and reinforcement details for the parameters considered in the case study. The cross-section of the rectangular column was 1,000 × 1,500 mm with longitudinal reinforcement of 32 Ø 32 mm bars. The longitudinal steel bars had yield strength of 420 MPa and were lap spliced at the column base. Transverse reinforcement for the column comprises rectangular hoops with a yield strength of 420 MPa. The cylinder compressive strength for the concrete used in the bridge substructure was 30 MPa. The lateral pushover analysis of the column was conducted keeping the axial load constant. The column was laterally displaced in the direction that produced moment about the strong axis of its cross-section. The parametric study incorporated the lap-splice length, volumetric ratio of hoop reinforcement, and the axial load ratio. The lap-splice length was varied between $20\phi_b$ and $60\phi_b$ (ϕ_b = bar-diameter); in addition to case of continuous longitudinal bars

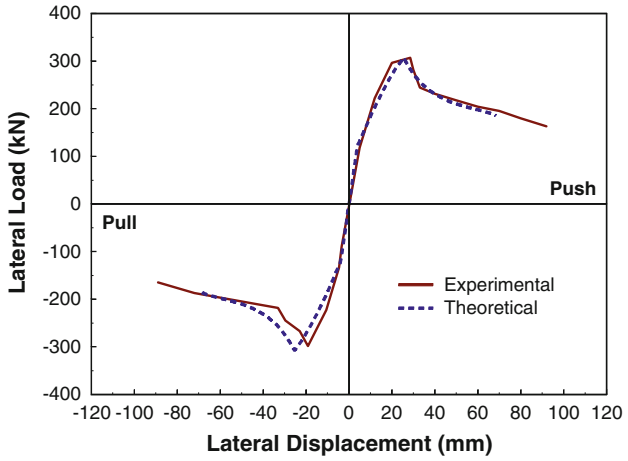

(a) Column RC(1)

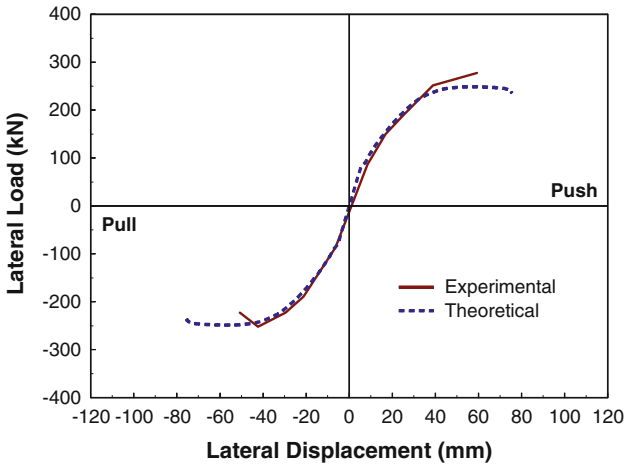

(b) Column RC(2)

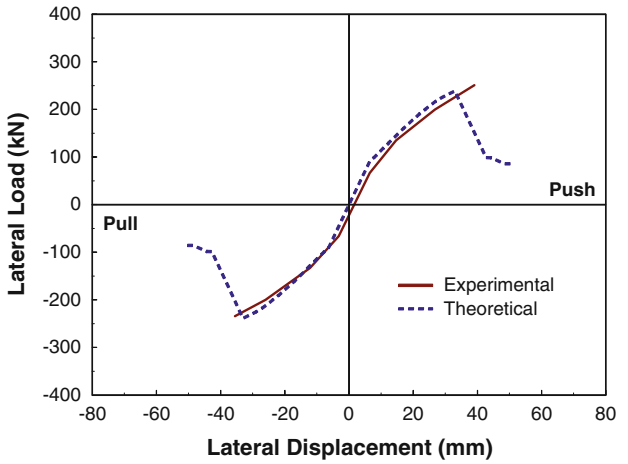

(c) Column RC(3)

Fig. 4 Comparison between load–displacement envelopes for columns **a** RC(1), **b** RC(2), **c** RC(2)

with no lap splice. The first three lengths ($20\phi_b$ to $40\phi_b$) represent the substandard lap splices, which were commonly utilized for the construction of many old bridges all over the world. The last two lengths $50\phi_b$ and $60\phi_b$, respectively, denote classes A and B tension splices as outlined by the ACI 318-11 code [1].

As seen in Fig. 5, six different volumetric ratios of hoop reinforcement were studied. The first volumetric ratio (ρ_v) of 0.12 % corresponds to substandard hoop details. The last ratio of 1.5 % corresponds to hoops required for columns to resist seismic loads as outlined in the seismic codes such as Caltrans design guidelines [2] and the ACI 318-11 code [1]. Last, nine different values were selected for the axial load ratio ($P/A_g f'_c$), ranging from 0.0 to 40 % as demonstrated in Table 3. The ratios between 5 and 20 % represent the most common bridge columns, whereas the ratios between 30 and 40 % correspond to columns with heavy axial loads as those found in special bridges and multistory buildings. Considering all these parameters, a total of 324 columns were analyzed in this study. Table 3 summarizes the details for all the analyzed columns along with the considered parameters.

4 Discussion and Analysis of Results

The results obtained from the pushover analysis conducted on the rectangular column specimens have been discussed in detail in the following sections.

4.1 Effect of Lap-Splice Length

4.1.1 Effect of Lap-Splice Length on Load–Displacement Curve

Figure 6a, b represents the effect of lap-splice length on the top lateral load–displacement curve of the columns for two cases of axial load ratios and with gravity load hoops with a volumetric ratio (ρ_v) of 0.29 %. The first graph represents the columns with an axial load ratio of 0.1, which is most common for bridge columns, whereas the second is for columns with an axial load ratio of 0.3, which is typical for columns in special bridges and multistory buildings. As seen in the figures, degradation in the post-peak lateral stiffness of the column due to bond deterioration of lap-spliced reinforcement is more pronounced with the lower axial load ratio (0.1). It is noticed that changes in the lap-splice length do not affect the pre-cracking stiffness, whereas the post-cracking stiffness increases as the lap-splice length increases. It is also noted that increasing the lap-splice length at the column

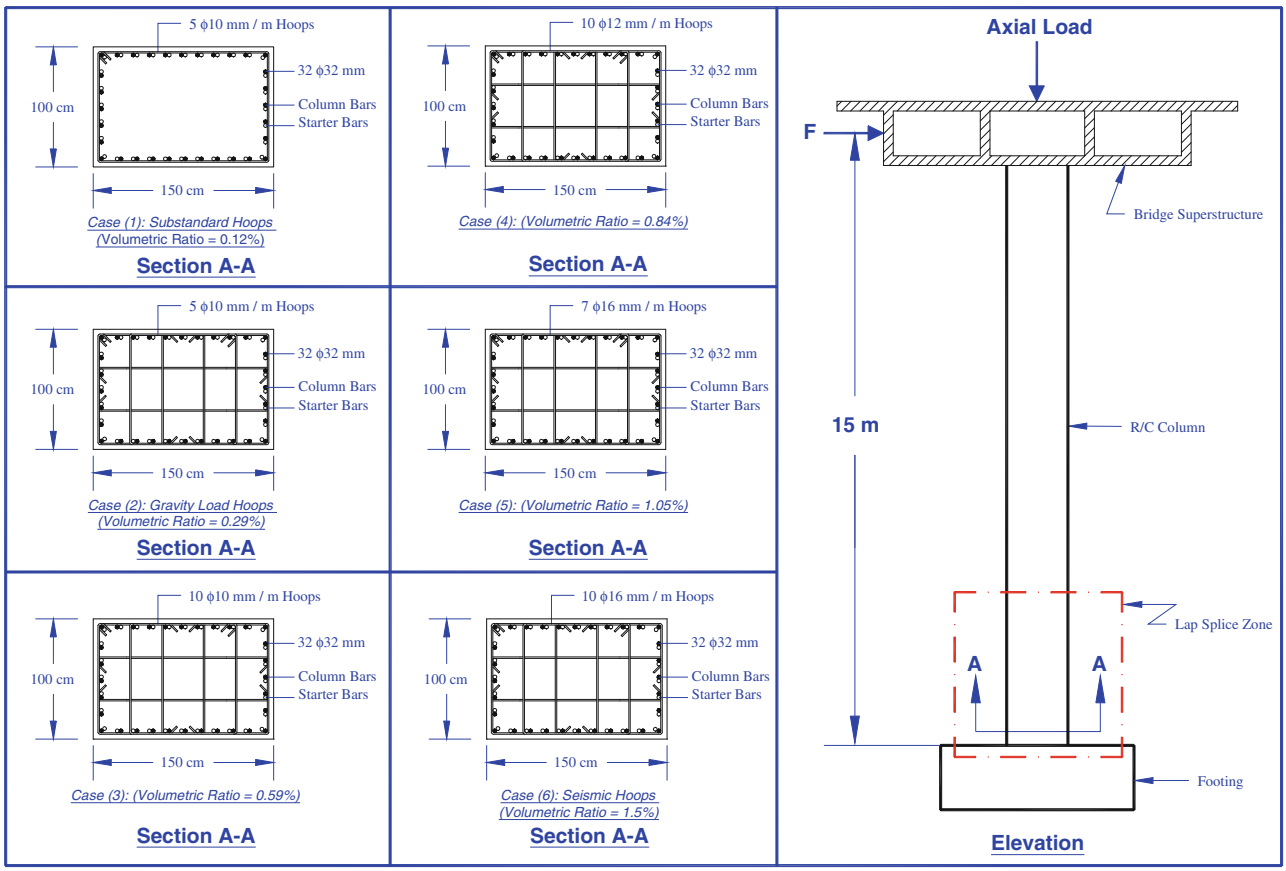

Fig. 5 Dimensions and reinforcement details of studied bridge columns

base enhances its top lateral load–displacement characteristics. Thereby, the column will have better energy absorption capacity when exposed to seismic (or blast) attacks. For axial load ratio of 0.1, post-peak stiffness degradation is noticed for lap lengths up to $40\phi_b$, after which no degradation occurs and the load–displacement response is the same for classes A and B tension splices and agrees very well with that for column with no lap splices. For the axial load ratio of 0.3, degradation in the post-peak lateral stiffness is observed for lap lengths up to $30\phi_b$, after which insignificant degradation occurs.

4.1.2 Effect of Lap-Splice Length on Flexural Strength of the Column

The maximum lateral load carrying capacity of a bridge column represents the level of flexural strength when exposed to seismic actions. Figure 7a, b illustrates for gravity load hoops and seismic hoops cases, respectively, the percentages of reduction in maximum lateral load due to lap splices for different axial load ratios. For the same hoop reinforcement and lap-splice length, as the axial load ratio increases the reduction in maximum lateral load decreases. For gravity load hoops ($\rho_v = 0.29\,\%$), as the lap-splice length increases the reduction in maximum lateral load decreases until a lap-splice length of $50\phi_b$ at which insignificant reduction in flexural strength occurs. However, for seismic hoops ($\rho_v = 1.5\,\%$), insignificant reduction in maximum lateral load occurs for columns with lap-splice length of $40\phi_b$ or more.

4.1.3 Effect of Lap-Splice Length on Column Displacement Ductility

Bridge substructures should have the capability to dissipate the energy absorbed from earthquakes or blast attacks without significant strength and stiffness degradation. Therefore, current bridge design guidelines (e.g., Caltrans design guidelines [2]) require the bridge columns to have a minimum displacement ductility of 4.0. In the present study, displacement ductility was computed for each column considered in this study and then plotted against lap-splice length ratio (L_s/ϕ_b) as seen in Fig. 8a, b for axial load ratios of 0.1 and 0.3, respectively. For columns with axial load ratio of 0.1,

Table 3 Details of studied columns

Column	Lap length (mm)	Type of lap splice	Axial load (kN)	Axial load ratio	Transverse hoops
C1 to C6	640	$20\phi_b$ (substandard splice)	0	0	Case 1: 5 Ø 10 mm/m
C7 to C12	960	$30\phi_b$ (substandard splice)	0	0	Exterior hoops with $\rho_v = 0.12\,\%$
C13 to C18	1,280	$40\phi_b$ (substandard splice)	0	0	(substandard volumetric ratio)
C19 to C24	1,600	$50\phi_b$ (ACI Class A tension splice)	0	0	
C25 to C30	1,920	$60\phi_b$ (ACI Class B tension splice)	0	0	
C31 to C36	No splices	None	0	0	
C37 to C42	640	$20\phi_b$ (substandard splice)	2,250	0.05	
C43 to C48	960	$30\phi_b$ (substandard splice)	2,250	0.05	
C49 to C54	1,280	$40\phi_b$ (substandard splice)	2,250	0.05	
C55 to C60	1,600	$50\phi_b$ (ACI Class A tension splice)	2,250	0.05	Case 2: 5 Ø10 mm/m
C61 to C66	1,920	$60\phi_b$ (ACI Class B tension splice)	2,250	0.05	Exterior and interior hoops with $\rho_v = 0.29\,\%$
C67 to C72	No splices	None	2,250	0.05	(satisfying ACI code provisions for gravity load requirements)
C73 to C78	640	$20\phi_b$ (substandard splice)	4,500	0.1	
C79 to C84	960	$30\phi_b$ (substandard splice)	4,500	0.1	
C85 to C90	1,280	$40\phi_b$ (substandard splice)	4,500	0.1	
C91 to C96	1,600	$50\phi_b$ (ACI Class A tension splice)	4,500	0.1	
C97 to C102	1,920	$60\phi_b$ (ACI Class B tension splice)	4,500	0.1	
C103 to C108	No splices	None	4,500	0.1	
C109 to C114	640	$20\phi_b$ (substandard splice)	6,750	0.15	Case 3: 10 Ø10 mm/m
C115 to C120	960	$30\phi_b$ (substandard splice)	6,750	0.15	Exterior and interior hoops with $\rho_v = 0.59\,\%$
C121 to C126	1,280	$40\phi_b$ (substandard splice)	6,750	0.15	
C127 to C132	1,600	$50\phi_b$ (ACI Class A tension splice)	6,750	0.15	
C133 to C138	1,920	$60\phi_b$ (ACI Class B tension splice)	6,750	0.15	
C139 to C144	No splices	None	6,750	0.15	
C145 to C150	640	$20\phi_b$ (substandard splice)	9,000	0.2	
C151 to C156	960	$30\phi_b$ (substandard splice)	9,000	0.2	
C157 to C162	1,280	$40\phi_b$ (substandard splice)	9,000	0.2	
C163 to C168	1,600	$50\phi_b$ (ACI Class A tension splice)	9,000	0.2	Case 4: 10 Ø12 mm/m
C169 to C174	1,920	$60\phi_b$ (ACI Class B tension splice)	9,000	0.2	Exterior and interior hoops with $\rho_v = 0.84\,\%$
C175 to C180	No splices	None	9,000	0.2	
C181 to C186	640	$20\phi_b$ (substandard splice)	11,250	0.25	
C187 to C192	960	$30\phi_b$ (substandard splice)	11,250	0.25	
C193 to C198	1,280	$40\phi_b$ (substandard splice)	11,250	0.25	
C199 to C204	1,600	$50\phi_b$ (ACI Class A tension splice)	11,250	0.25	
C205 to C210	1,920	$60\phi_b$ (ACI Class B tension splice)	11,250	0.25	
C211 to C216	No splices	None	11,250	0.25	
C217 to C222	640	$20\phi_b$ (substandard splice)	13,500	0.3	
C223 to C228	960	$30\phi_b$ (substandard splice)	13,500	0.3	Case 5: 7 Ø16 mm/m
C229 to C234	1,280	$40\phi_b$ (substandard splice)	13,500	0.3	Exterior and interior hoops with $\rho_v = 1.05\,\%$
C235 to C240	1,600	$50\phi_b$ (ACI Class A tension splice)	13,500	0.3	
C241 to C246	1,920	$60\phi_b$ (ACI Class B tension splice)	13,500	0.3	
C247 to C252	No splices	None	13,500	0.3	
C253 to C258	640	$20\phi_b$ (substandard splice)	15,750	0.35	
C259 to C264	960	$30\phi_b$ (substandard splice)	15,750	0.35	
C265 to C270	1,280	$40\phi_b$ (substandard splice)	15,750	0.35	
C271 to C276	1,600	$50\phi_b$ (ACI Class A tension splice)	15,750	0.35	

Table 3 continued

Column	Lap length (mm)	Type of lap splice	Axial load (kN)	Axial load ratio	Transverse hoops
C277 to C282	1,920	$60\phi_b$ (ACI Class B tension splice)	15,750	0.35	Case 6: 10 Ø16 mm/m
C283 to C288	No splices	None	15,750	0.35	Exterior and interior hoops with $\rho_v = 1.5\,\%$
C289 to C294	640	$20\phi_b$ (substandard splice)	18,000	0.4	(satisfying ACI code provisions for seismic load requirements)
C295 to C300	960	$30\phi_b$ (substandard splice)	18,000	0.4	
C301 to C306	1,280	$40\phi_b$ (substandard splice)	18,000	0.4	
C307 to C312	1,600	$50\phi_b$ (ACI Class A tension splice)	18,000	0.4	
C313 to C318	1,920	$60\phi_b$ (ACI Class B tension splice)	18,000	0.4	
C319 to C324	No splices	None	18,000	0.4	

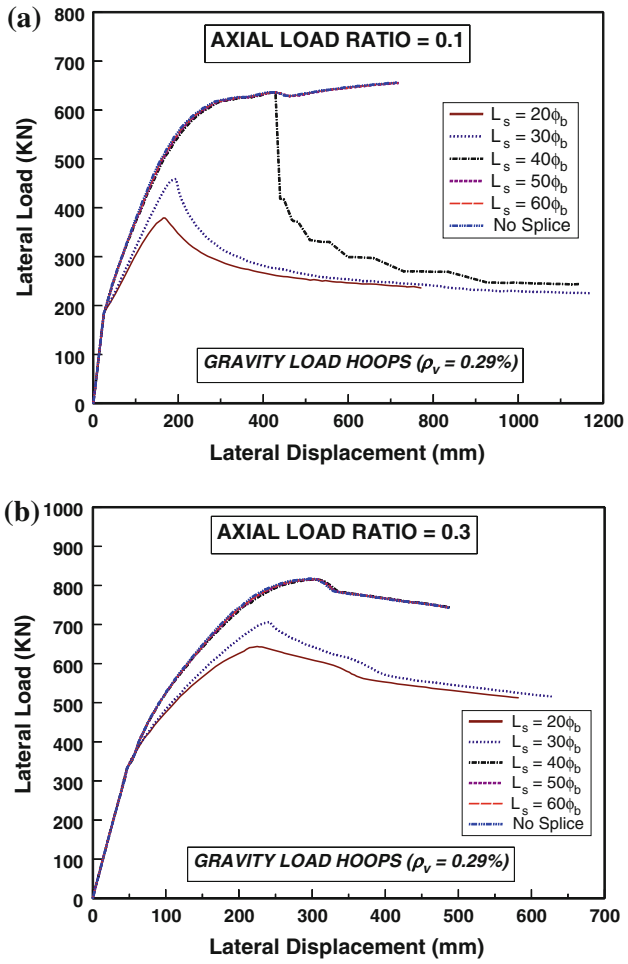

Fig. 6 Effect of lap-splice length on load–displacement curve

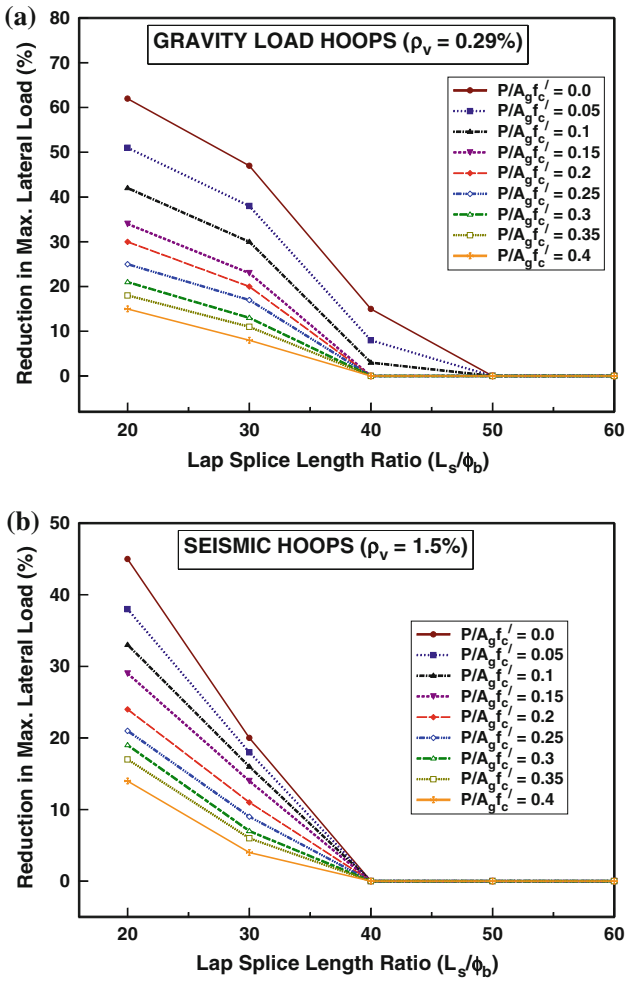

Fig. 7 Effect of lap-splice length on reduction of maximum lateral load

as the lap-splice length increases the displacement ductility increases until a lap length of $50\phi_b$ after which the increase in the ductility became insignificant. For columns with axial load ratio of 0.3, as the lap-splice length increases the displacement ductility increases until a lap length of $40\phi_b$ after which insignificant increase in ductility was noted. For the two cases of axial load ratios, in order to achieve a minimum displacement ductility of 4.0, lap splices as short as $20\phi_b$

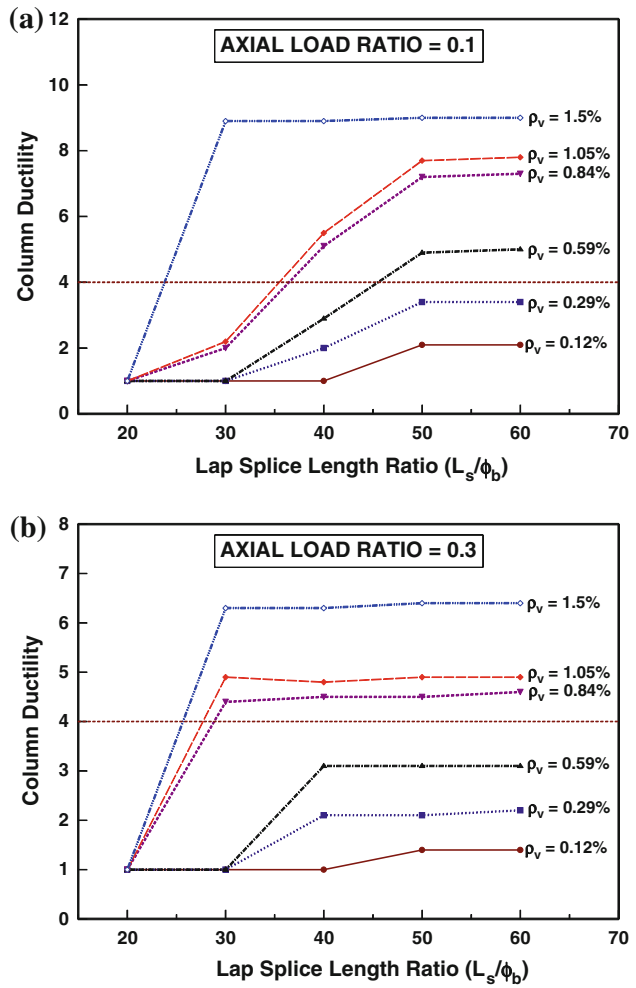

Fig. 8 Effect of lap-splice length on column ductility

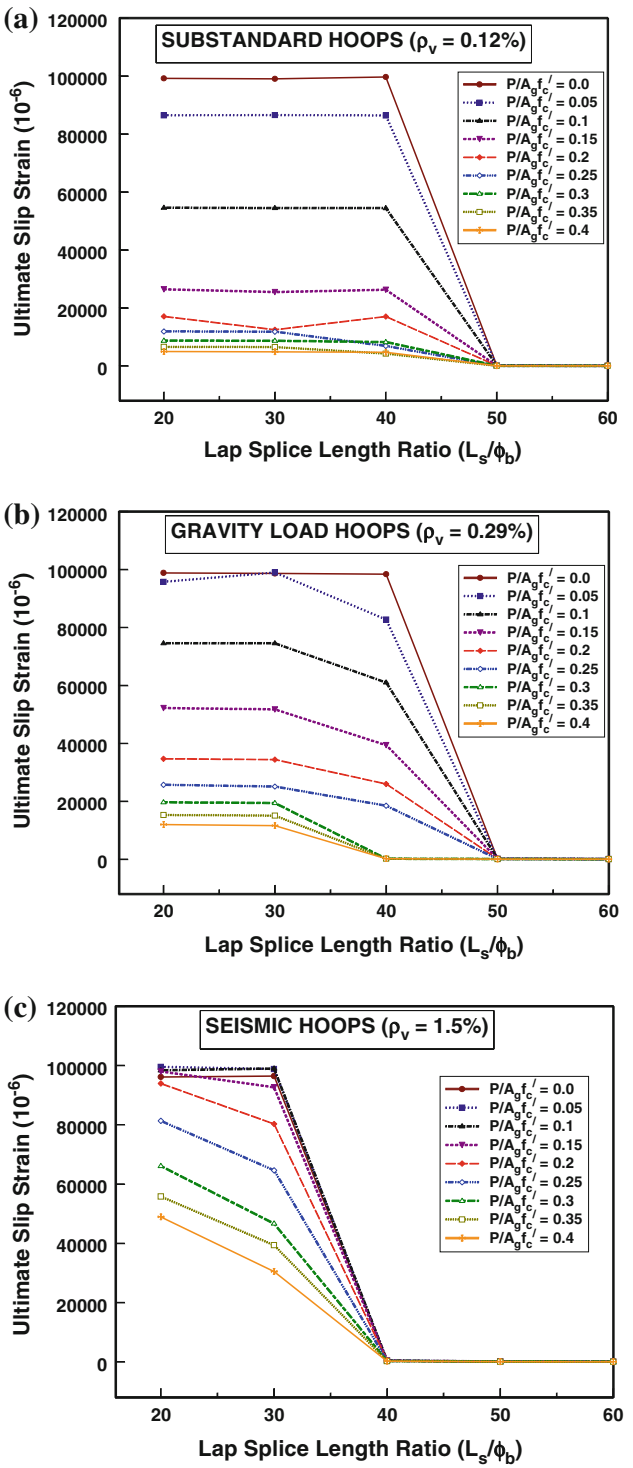

Fig. 9 Effect of lap-splice length on ultimate slip strain

and $30\phi_b$ should not be used in the potential plastic hinge locations.

4.1.4 Effect of Lap-Splice Length on Ultimate Slip Strain of Longitudinal Tension Bars

For a fully effective bond between reinforcing steel and surrounding concrete, no slippage should occur and the bar slip strain should be near zero. Higher slip strains are usually anticipated for short lap splices and always induce large column deformations; however, it does not necessarily lead to stiffness degradation unless poor lap-splice clamping is provided. Ultimate slip strain of the extreme tension bars in the column section was computed and then plotted against the lap-splice length ratio (L_s/ϕ_b) as demonstrated in Fig. 9a–c for three different levels of hoop reinforcement ($\rho_v = 0.12$, 0.29 and 1.5 %). As shown in the graphs, increasing the axial load ratio significantly reduces the ultimate slip strain, especially for columns with low levels of hoop reinforcement. For classes A and B tension splices, very small slip strains were observed for different levels of both axial load ratio and hoop reinforcement. However, for a lap splice with a length of $40\phi_b$, very small slip strains were calculated only, for columns with seismic hoops ($\rho_v = 1.5$ %).

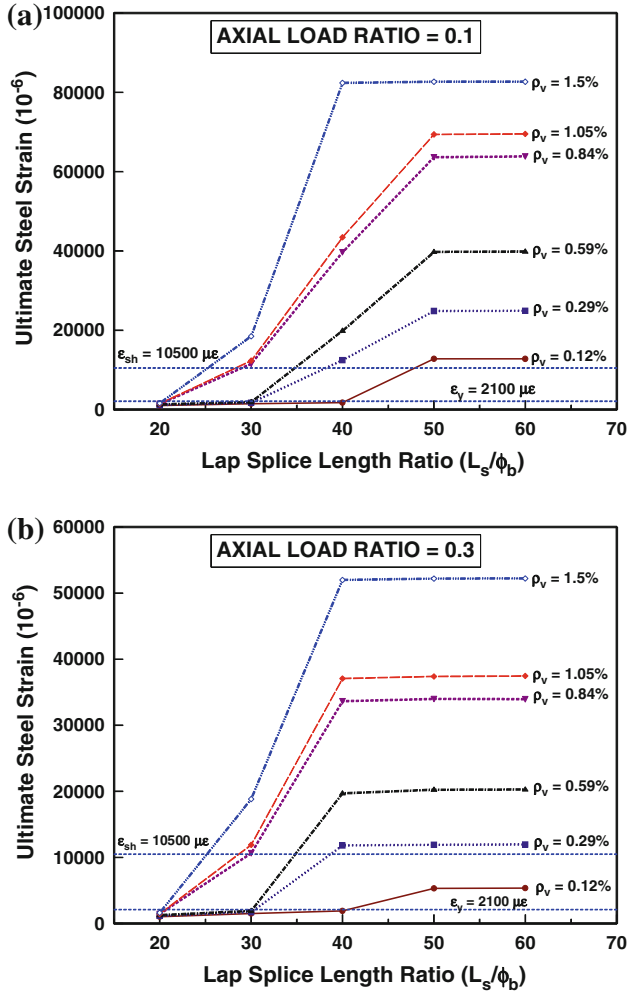

Fig. 10 Effect of lap-splice length on ultimate tensile steel strain

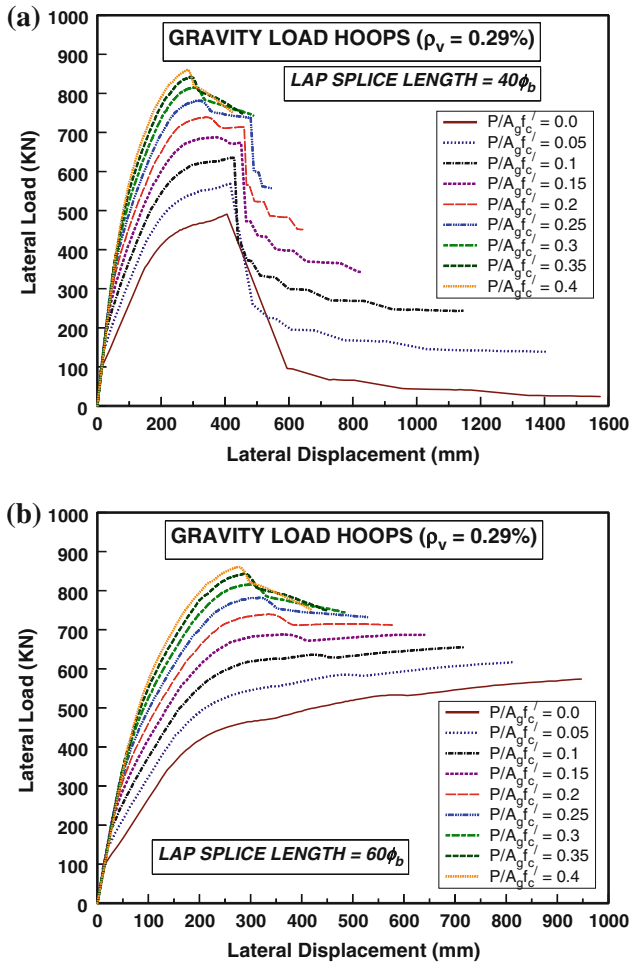

Fig. 11 Effect of axial load ratio on load–displacement curve

4.1.5 Effect of Lap-Splice Length on Ultimate Elongation Strain of Longitudinal Tension Bars

As mentioned earlier, the total geometric strain for each bar in tension consists of two components: slippage and elongation. Figure 10a, b shows the plots for the ultimate elongation strains calculated for the extreme tension bars in the column cross section, plotted against lap-splice length ratio (L_s/ϕ_b), for the axial load ratios of 0.1 and 0.3, respectively. On the graphs, the yield strain, ε_y, and the strain at onset of strain hardening, ε_{sh}, are shown for reference. For columns with an axial load ratio of 0.1, as the lap-splice length increases the ultimate tensile steel strain increases until a lap length of $50\phi_b$ after which no increase in ultimate steel strain takes place. For columns with axial load ratio of 0.3, as the lap-splice length increases the ultimate tensile steel strain increases up to a lap length of $40\phi_b$ after which insignificant increase in ultimate steel strain occurs. In columns with lap-splice length of $20\phi_b$, it was noticed that the tensile steel did not even reach the yield point. However, in columns with lap-splice length of $30\phi_b$, tensile steel entered the strain-hardening zone with transverse hoops of minimum volumetric ratio of 0.84 %.

4.2 Effect of Axial Load Ratio

4.2.1 Effect of Axial Load Ratio on Load–Displacement Curve

The effect of axial load ratio on load–displacement curves is demonstrated in Fig. 11a, b for lap lengths of $40\phi_b$ and $60\phi_b$, respectively. The graphs are shown for hoops of volumetric ratio of 0.29 %, which corresponds to those used in gravity-loaded columns. For lap-splice length of $40\phi_b$, it is noted that increasing the axial load on the column retards bond slippage of lap-spliced reinforcement until higher stages of lateral loading. For both cases, it was found that increasing the axial load on the column not only increases its flexural strength and lateral stiffness (post-cracking slope of load–

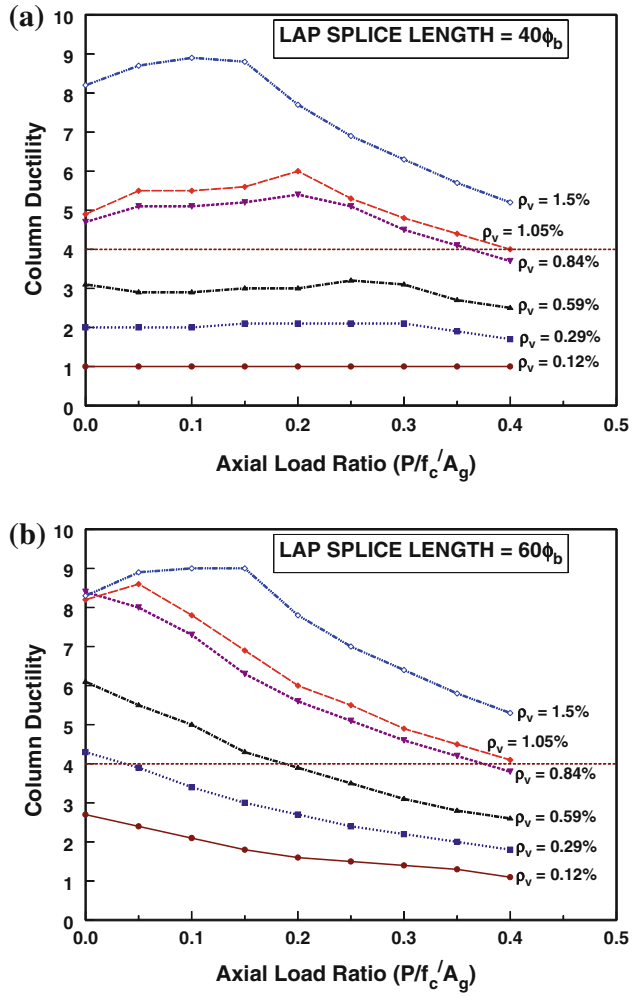

Fig. 12 Effect of axial load ratio on column ductility

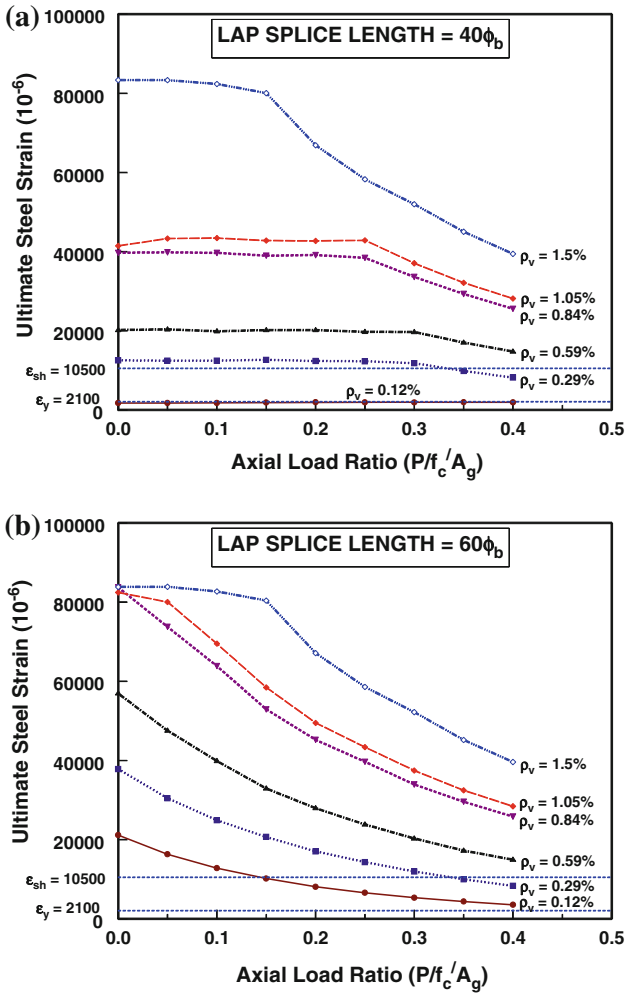

Fig. 13 Effect of axial load ratio on ultimate tensile steel strain

displacement curve) but also decreases its ultimate lateral displacement.

4.2.2 *Effect of Axial Load Ratio on Column Displacement Ductility*

The effect of axial load ratio on column ductility is demonstrated in Fig. 12a, b for lap lengths of $40\phi_b$ and $60\phi_b$, respectively. For lap-splice length of $40\phi_b$, increasing the axial load ratio has insignificant effect on the column ductility for columns with transverse hoops of volumetric ratios up to 0.59 %. Yet, for columns with transverse hoops of minimum volumetric ratio of 0.84 %, increasing the axial load ratio beyond 20 % decreases the displacement ductility of the column. For columns with Class B tension splices (lap length = $60\phi_b$), increasing the axial load ratio generally reduces the displacement ductility. For columns with lap-splice length of $40\phi_b$ or more and subjected to low or moderate levels of axial load ratio (up to 20 %), transverse hoops with minimum volumetric ratio of 0.84 % should be provided within the lap-splice zone. And, for columns with high levels of axial load ratio (30–40 %), the lap-splice region should be confined with hoop reinforcement of a minimum volumetric ratio of 1.05 %.

4.2.3 *Effect of Axial Load Ratio on Ultimate Elongation Strain of Longitudinal Tension Bars*

The effect of axial load ratio on the ultimate tensile steel strain is demonstrated in Fig. 13a, b for lap lengths of $40\phi_b$ and $60\phi_b$, respectively. In general, increasing the axial load ratio reduces the ultimate tensile steel strain, especially for columns with Class B tension splice. For columns with lap-splice length of $40\phi_b$ or more and subjected to low or moderate levels of axial load ratio (up to 20 %), transverse hoops with a minimum volumetric ratio of 0.29 % should be provided within the lap-splice zone in order for the extreme tension bars to go into the strain-hardening zone. However,

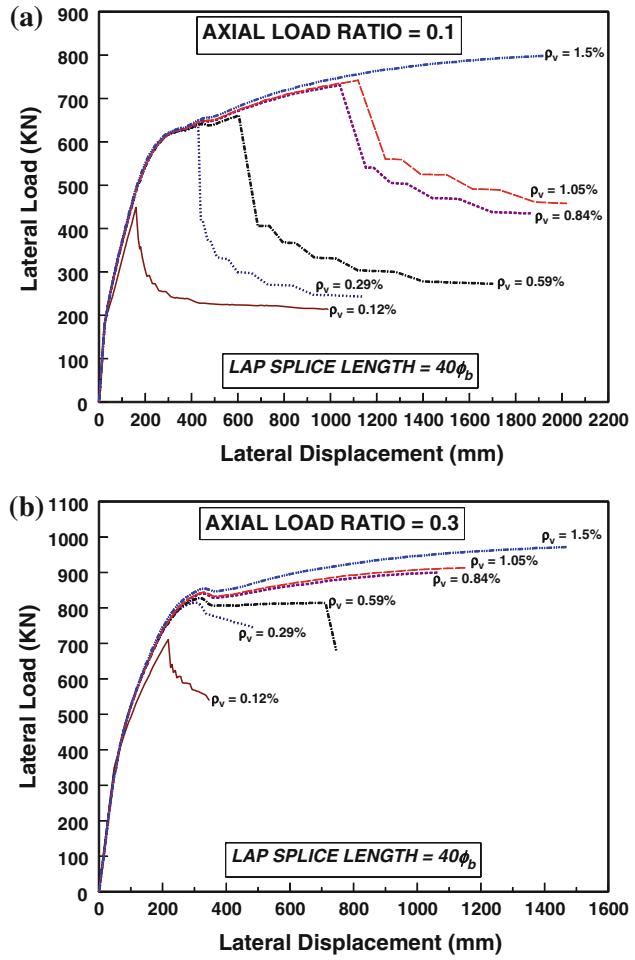

Fig. 14 Effect of volumetric ratio of column hoops on load–displacement curve

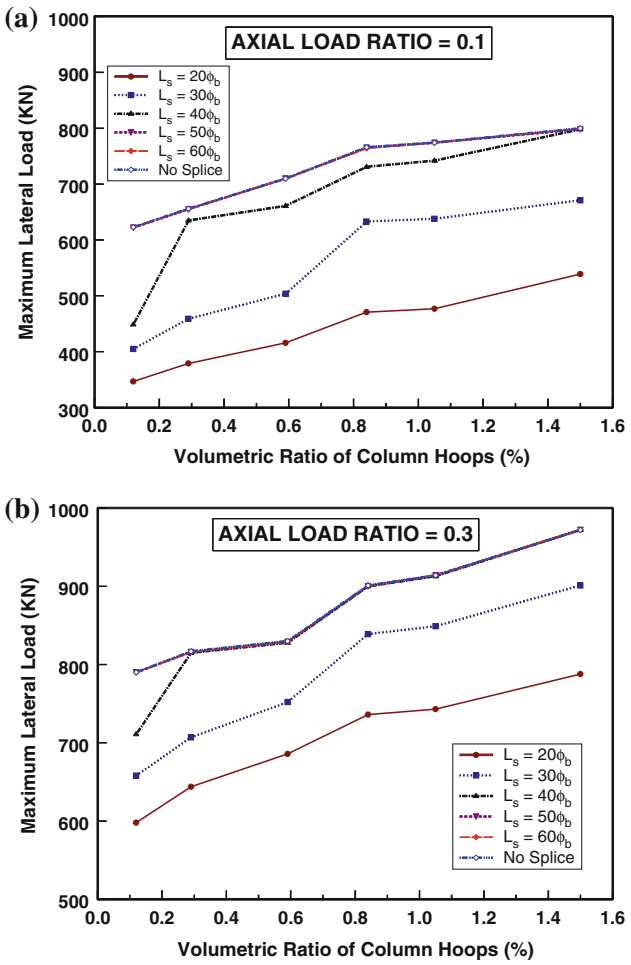

Fig. 15 Effect of volumetric ratio of column hoops on maximum lateral load

strain hardening occurs for extreme tension bars in columns with high levels of axial load ratio (30–40 %) when the lap-splice region is confined with hoop reinforcement of minimum volumetric ratio of 0.59 %.

4.3 Effect of Transverse Hoops Ratio

4.3.1 Effect of Transverse Hoops Ratio on Load–Displacement Curve

Presented in Fig. 14a, b is the effect of volumetric ratio of transverse hoops on load–displacement behavior of columns with axial load ratios of 0.1 and 0.3, respectively. The graphs are shown for columns with lap-splice length of $40\phi_b$. In general, increasing the volumetric ratio of transverse hoops improves the load–displacement response of the column. For axial load ratio of 0.1, post-peak stiffness degradation is observed for all hoop ratios except for seismic hoops ($\rho_v = 1.5\,\%$) for which no stiffness degradation occurs. However, for axial load ratio of 0.3, no stiffness degradation occurs for columns having transverse hoops of volumetric ratio greater than 0.59 %.

4.3.2 Effect of Transverse Hoops Ratio on Column Flexural Strength

Presented in Fig. 15a, b, respectively, are the effects of volumetric ratio of column hoops, for the axial load ratios of 0.1 and 0.3, on the maximum lateral load for different lap-splice lengths. For the same lap-splice length, increasing the volumetric ratio of column hoops improves its flexural strength due to hoop effectiveness on enhancing both concrete confinement and lap-splice clamping. This may bring attention to the importance of hoop reinforcement in reinforced concrete columns subjected to lateral loading. By paying attention to the transverse hoops in terms of volumetric ratio (amount and spacing), flexural strength enhancement may be gained without increasing the dimensions of the cross section, especially for bridge columns located in low seismic regions. Increasing the dimensions of the column section is not always desirable

as it may cause an increase in the stiffness thereby attracting higher seismic forces and alteration of bridge dynamic characteristics. For an axial load ratio of 0.1, as the lap-splice length increases from $20\phi_b$ to $50\phi_b$, the maximum lateral load also increases. The flexural strength is the same for classes A and B tension splices and approximately comes to that for columns with no lap splices. For an axial load ratio of 0.3, increase in flexural strength is observed for lap lengths up to $40\phi_b$, after which insignificant increase in maximum lateral load takes place and the flexural strength is the same for columns with lap-splice length of $40\phi_b$ or more.

5 Conclusions

The following conclusions are derived from the results of this research:

1. The top lateral load–displacement characteristics of a column and thereby its energy absorption capacity when exposed to lateral loading as a result of seismic loads (or blast attacks) can be improved by increasing the lap-splice length at the column base.
2. In order to achieve a minimum ductility of 4.0 as required by current seismic design guidelines for bridges (such as Caltrans design guidelines), lap splices as short as $20\phi_b$ and $30\phi_b$ should not be used in the potential plastic hinge locations.
3. For the same lap-splice length, increasing the volumetric ratio of column hoops enhances the lateral load–displacement response due to the hoops effectiveness on enhancing both concrete confinement and lap-splice clamping.
4. Increasing the axial load on the column delays bond slippage in the tension lap splice until higher stages of lateral loading.
5. Increasing the axial load on the column increases its flexural strength and post-cracking lateral stiffness.
6. Increasing the axial load on the column decreases its ultimate lateral displacement and ductility.
7. For R/C tall rectangular bridge columns with low (or moderate) levels of axial load ratio (up to 20 %) and subjected to low (or moderate) seismic actions, lap splices, if used in the plastic hinge locations, have to be at least of the ACI's Class A type tension splice and should be clamped with hoop reinforcement of at least 50 % of that required by the ACI code for seismic design. However, if the columns shall experience strong seismic actions (or blast attacks), seismic hoops as required by the ACI code should be provided within the lap-splice region.
8. For R/C tall rectangular bridge columns with high levels of axial load ratio (30–40 %) and subjected to low (or moderate) seismic actions, lap splices, if used in the potential plastic hinge locations, have to be at least of $40\phi_b$ length and should be confined with hoop reinforcement of at least 70 % of that required by the ACI code for seismic design. Yet, if the columns shall experience strong seismic actions (or blast attacks), seismic hoops as required by the ACI code should be used in the lap-splice zone.

Acknowledgments The authors gratefully acknowledge the support by the Specialty Units for Safety and Preservation of Structures and the Saudi Aramco Chair for Earthquake Engineering (SACEE), Department of Civil Engineering, King Saud University.

References

1. ACI Committee 318: Building Code Requirements for Reinforced Concrete and Commentary, ACI 318-11. American Concrete Institute, Farmington Hills (2011)
2. Caltrans: Seismic Design Criteria. Version 1.6, Sacramento, California, November (2010)
3. Sun, Z.L.; Seible, F.; Priestley, M.J.N.: Flexural Retrofit of Rectangular Reinforced Concrete Bridge Columns by Steel Jacketing—Experimental Studies. In: Structural Systems Research Project, Report No. SSRP—93/01. Department of Applied Mechanics and Engineering Sciences, University of California, San Diego, La Jolla, California, February (1993)
4. Chung, Y.S.; Lee, J.H.; Kim, Y.: Seismic Performance and retrofit of circular bridge piers with spliced longitudinal steel. KCI Concr. J. **14**(3), 130–137 (2002)
5. Kim, T.H.; Kim, B.S.; Chung, Y.S.; Shin, H.M.: Seismic performance assessment of reinforced concrete bridge piers with lap splices. Eng. Struct. J. **28**, 935–945 (2006)
6. Chung, Y.S.; Park, C.K.; Meyer, C.: Residual seismic performance of reinforced concrete bridge piers after moderate earthquakes. ACI Struct. J. **105**(1), 87–95 (2008)
7. Elsanadedy, H.M.: Seismic Performance and Analysis of Ductile Composite-Jacketed Reinforced Concrete Bridge Columns. Ph.D. Dissertation, University of California, Irvine (2002)
8. Haroun, M.A.; Elsanadedy, H.M.: Fiber-reinforced plastic jackets for ductility enhancement of reinforced concrete bridge columns with poor lap-splice detailing. J. Bridge Eng. ASCE **10**, 749–757 (2005)
9. Bousias, S.; Spathis, A.L.; Fardis, M.N.: Seismic retrofitting of columns with lap-splices through CFRP jackets. In: 13th World Conference on Earthquake Engineering, Paper No. 765. Vancouver, Canada, August (2004)
10. Bousias, S.; Spathis, A.L.; Fardis, M.N.: Seismic retrofitting of columns with lap-splices via RC Jackets. 13th World Conference on Earthquake Engineering, Paper No. 1937. Vancouver, Canada, August (2004)
11. Chang, K.C.; Chung, L.L.; Lee, B.J.; Li, Y.F.; Tsai, K.C.; Hwang, J.S.; Hwang, S.J.: Seismic retrofit study of RC bridge columns. In: International Training Programs for Seismic Design on Building Structures. National Center for Research on Earthquake Engineering (NCREE), Taipei, Taiwan. January (2002)
12. Chang, K.C.; Lin, K.Y.; Cheng, S.B.: Seismic retrofit study of RC rectangular bridge columns lap-spliced at the plastic hinge zone. In: Proceedings of the International Conference of FRP Composites in Civil Engineering, pp. 869–875. Hong Kong, China (2001)
13. ElGawady, M.; Endeshaw, M.; McLean, D.; Sack, R.: Retrofitting of rectangular columns with deficient lap splices. J. Compos. Constr. ASCE **14**, 22–35 (2010)

14. Ghosh, K.K.; Sheikh, S.A.: Seismic upgrade with carbon fiber-reinforced polymer of columns containing lap-spliced reinforcing bars. ACI Struct. J. **104**(2), 227–236 (2007)
15. Xiao, Y.; Rui, M.: Seismic retrofit of RC circular columns using prefabricated composite jacketing. J. Struct. Eng. ASCE **123**(10), 1357–1364 (1997)
16. Mander, J.B.; Priestley, M.J.N.; Park, R.: Theoretical stress–strain model for confined concrete. J. Struct. Div. ASCE **114**(8), 1804–1826 (1988)
17. Priestley, M.J.N.; Seible, F.; Calvi, G.M.: Seismic Design and Retrofit of Bridges. Wiley, New York (1996)
18. ACI Committee 408: Bond and Development of Straight Reinforcing Bars in Tension. ACI 408R-03. American Concrete Institute, Farmington Hills (2003)
19. Melek, M.; Wallace, J.W.: Performance of columns with short lap splices. In: 13th World Conference on Earthquake Engineering, Vancouver, B.C., Canada, (2004)